



Contents lists available at ScienceDirect

Materials Today: Proceedings

journal homepage: www.elsevier.com/locate/matpr

Molecular docking and antioxidant activity of *Cleome simplicifolia* assisted synthesis of cerium oxide nanoparticles

Ratiram Gomaji Chaudhary^{a,*}, Prashant B. Chouke^{a,b,*}, Rina D. Bagade^c, Ajay K. Potbhare^a, Kanhaiya M. Dadure^{d,*}

^a Post Graduate Department of Chemistry, Seth Kesarimal Porwal College, Kamptee 441 001, India

^b Department of Chemistry, Government Polytechnic, Bramhapuri 441 206, India

^c Post Graduate Teaching Department of Chemistry, Rashtrasant Tukadoji Maharaj Nagpur University, Nagpur 440033, India

^d Department of Chemistry, J. B. Science College, Wardha 442001, India

ARTICLE INFO

Article history:

Received 26 April 2020

Received in revised form 1 May 2020

Accepted 3 May 2020

Available online xxxx

Keywords:

Green-motivated CeO₂ NPs

Cleome simplicifolia

Microscopy techniques

Antioxidant assay

Molecular docking

ABSTRACT

Bio-motivated CeO₂ NPs were fabricated using plant extract of *Cleome simplicifolia*. The chemicals present in the plant extracts played pivotal role in the fabrication of CeO₂ NPs. Initially, fabricated CeO₂ nanoparticles were authenticated by using the XRD pattern which resembles a cubic structure. UV-Visible data estimated the band gap of CeO₂ around 3.50 eV. SEM images revealed nearly monodisperse spherical shapes due to agglomeration of CeO₂ NPs. DPPH assay of CeO₂ NPs exhibited an excellent antioxidant property. Moreover, molecular docking of CeO₂ NPs was investigated by new protein molecule.

© 2020 Elsevier Ltd. All rights reserved.

Selection and peer-review under responsibility of the scientific committee of the International Conference on Advanced Functional Materials (Innovations in Chemical, Physical and Biological Sciences).

1. Introduction

Nowadays, a synthesis of bio-coherent metal/metal oxide nanoparticles and semiconductor nano-structure is a significant part in the field of science and technology. Recently, cerium oxide nanoparticles (CeO₂ NPs) have been immensely utilized as semiconducting materials with wide band gap energy 3.50 eV. CeO₂ NPs are capable in showing the applications in various fields viz. drug delivery, agriculture, pharmaceuticals and biosensor [1–5]. Earlier, a variety of synthesis techniques has been employed to fabricate the CeO₂ NPs such as sol-gel [6], co-precipitation [7], microwave [8], hydrothermal [9], flame spray pyrolysis [10], and sonochemical [11]. However, the applied methods are compact with several negative aspects such as very expensive, use hazardous chemical, toxicity, complicated, time-consuming and harmful to perform [12]. In response, researchers are searching for alternatives to conventional methods. “Green approach” has a

capacity to minimize the elimination of harmful gases and chemicals during the formation of NPs [13]. The green method possesses abundant benefits such as low-cost, eco-friendly, large scale production on a commercial basis and a lot of biomedical applications [14,15].

Therefore, we referred the various kinds of literatures concerning cerium oxide NPs and found that, cerium is the first rare earth metal of lanthanide series in the periodic table. Cerium can be present in both 3⁺ and 4⁺ states. Therefore, in a bulk condition cerium oxide can be in existence as both CeO₂ and Ce₂O₃. At nanoscale, cerium oxide reveals a mix of cerium in the 3⁺ and 4⁺ states on the surface of the nanoparticles [16]. As a result, CeO₂ NPs are being extensively used in nanotechnology due to their helpful applications as catalysts, fuel cells, and antioxidants in biological systems [17–21]. Hence, CeO₂ NPs have been synthesized by using many bio-components such as fungal extracellular, honey and white egg. These bio-components, behaving like stabilizing and anti-oxidizing agents cause to manufacture crystalline structure of NPs with different shape, size, and morphology. Such observed things inspired us to do something new. Thus, we have adopted a green approach to synthesize CeO₂ NPs by using plant extracts of *Cleome simplicifolia* and its antioxidant properties have been reported for the first time here.

* Corresponding authors at: Post Graduate Department of Chemistry, Seth Kesarimal Porwal College, Kamptee 441 001, India (P.B. Chouke).

E-mail addresses: chaudhary_rati@yahoo.com (R. Gomaji Chaudhary), prashant_bchouke@rediffmail.com (P.B. Chouke), kmdadure@gmail.com (K.M. Dadure).

<https://doi.org/10.1016/j.matpr.2020.05.062>

2214-7853/© 2020 Elsevier Ltd. All rights reserved.

Selection and peer-review under responsibility of the scientific committee of the International Conference on Advanced Functional Materials (Innovations in Chemical, Physical and Biological Sciences).

The *Cleome simplicifolia* existed in *Cleomaceae* family. The plant is about 15 to 60 cm tall, annual herb and native of Asia. This plant can be observed in the parts of Andhra Pradesh, Chhattisgarh, Goa, Gujarat, Karnataka, and prominently found in the part of Maharashtra. The plant is collected from the western part of Nagpur. Every part of the plant has been used in medicine. The plant is being used as a traditional medicine by the tribal's. Earlier, many researchers reported the bioinspired synthesis of CeO₂ nanoparticles using *Curvularia lunata* [22], *Olea europaea* [23], *Aloe arbadensis* [24], and *Hibiscus Sabdariffa* [25].

In the present study, we have carried out bio-assisted synthesized CeO₂ NPs using plant extract of *Cleome simplicifolia*. After fabrication, CeO₂ NPs were confirmed by different microscopic techniques. On the other hand, we have studied the antioxidant property of fabricated CeO₂ NPs. Similarly, we have also studied how protein (enzyme) interacts with a molecule (Ligand) of synthesised CeO₂ NPs under molecular docking. This is the first report on *Cleome simplicifolia* assisted green synthesis of CeO₂ NPs.

2. Materials and methods

2.1. Chemicals reagents

Cerium nitrate hexahydrate Ce(NO₃)₃·6H₂O with purity 99%, procured from Merck, where as 1-Diphenyl-2-picrylhydrazyl (DPPH) was purchased from Himedia laboratories. Without any purification all chemicals were used to carry out the experiments.

2.2. Fabrication of leaves extract

In the present work, *Cleome simplicifolia* was collected from Gorewada National Park, Nagpur, India. The plant was recognized with the support of taxonomists. The plant was cleaned several times using potable water, again with sterilised water to eliminate the surface contamination and soil present on the plant. Subsequently cleaned plant pieces were shadow dried for 5 to 6 days, then the dehydrated plant was cut into fine particles and make a powdered with the help of mortar and pistol. An aqueous solution of the plant was prepared by mixing 20 g of sterile fine particles of plant in 300 mL distilled water, boiled at 60 °C for 30 min and later the solution was cleaned by Whatman filter paper No.42 to take away the undesirable materials. Then, the solution was centrifuged at 3000 rpm for 3 min whereas the supernatant was used for fabrication of nanoparticles.

2.3. Bioinspired synthesis of cerium oxide NPs (CeO₂ NPs)

0.86 g of cerium nitrate hexahydrate (Ce (NO₃)₃·6H₂O) was suspended in 200 mL water, where 20 mL extract was added dropwise and stirred the mixture for half an hour by using a magnetic stirrer. Green colour precipitate in a conical flask at the bottom was obtained. The volume of supernatant liquid was removed from the conical flask to concentrate the obtained product as a precipitant. The obtained precipitant was washed thoroughly with sterilised water repeatedly, followed by alcohol and later dried it in an oven at 80 °C to acquire the very well particles of CeO₂ NPs. Further, the dried precipitate was calcinated at 800 °C for 2 h (Scheme 1).

2.4. Spectroscopic instrumentation for CeO₂ NPs

The intense peak of CeO₂ NPs was investigated with the help of lambda 35 UV-Visible Spectroscopy. JASCO 460 PLUS FTIR spectrometer was used to determine the IR spectra in the region of 4000–400 cm⁻¹. Cu K α radiation ($\lambda = 1.54060 \text{ \AA}$) with nickel monochromator was used to record the XRD pattern of fabricated

NPs in the region of 2θ from 10° to 80°. Scherrer's formula [$D = 0.9\lambda/\beta\cos\theta$] was employed to determine the standard crystallite size of material. The morphology of material was examined by JEOL JSM-7100 F instruments.

2.5. Antioxidant activity

The reducing capability of the CeO₂ nanoparticles was examined by a DPPH free radical scavenging technique according to our previous work [26]. Near about 10 to 50 μg of CeO₂ nanoparticles was mixed to 100 μL of DPPH solution. Afterwards the reaction mixture was incubated for 30 min at room temperature where the absorbance (A) was recorded at 517 nm using a spectrophotometer. This procedure was repeated for three times. Here, ascorbic acid was employed as a standard material. At last scavenging measurement of free radicals was calculated as % inhibition according to the standard formula.

2.6. Docking study

The 2-D and 3-D structures of these molecules were designed by using Chem Office software 12. The process of 2D and 3D design is elaborately explained in the user manual of the Chem Office and was used here without any modifications. CHIMERA and PYMOL tools were used to visualize the docked site.

3. Results and discussion

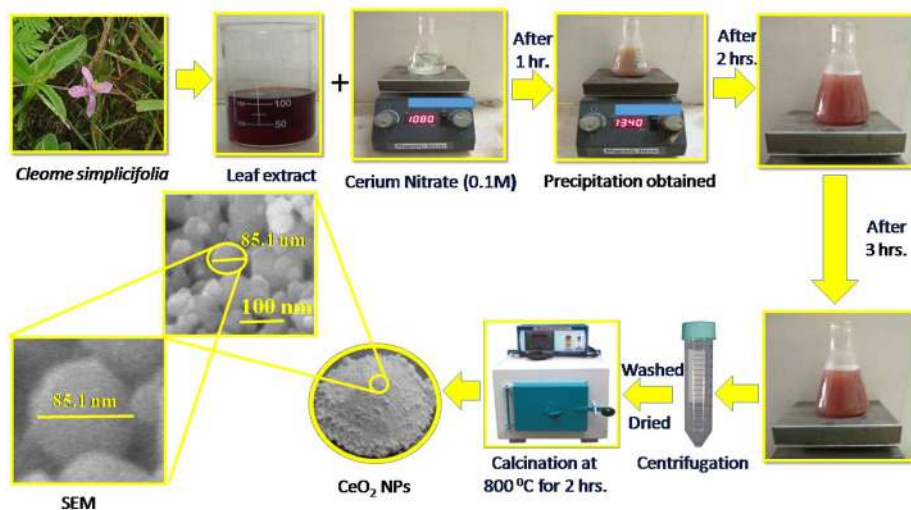
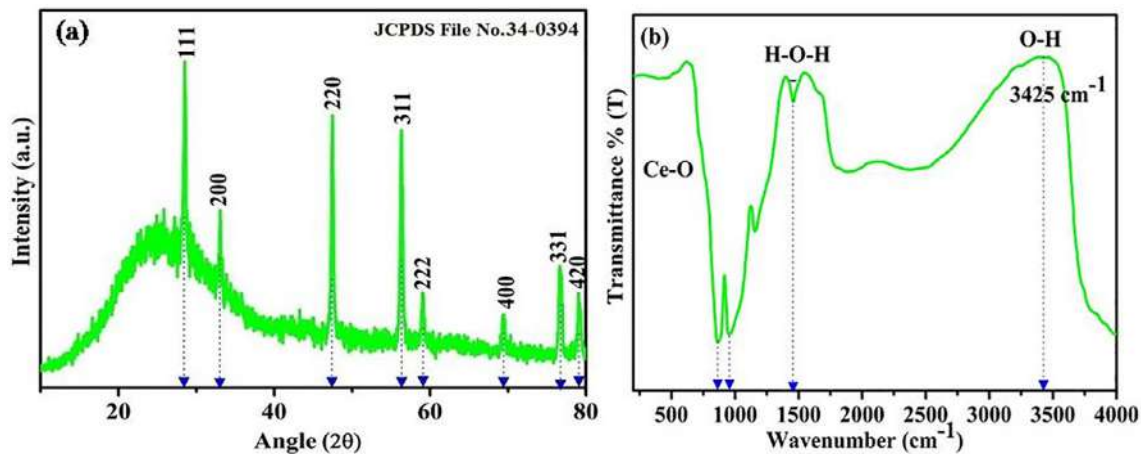
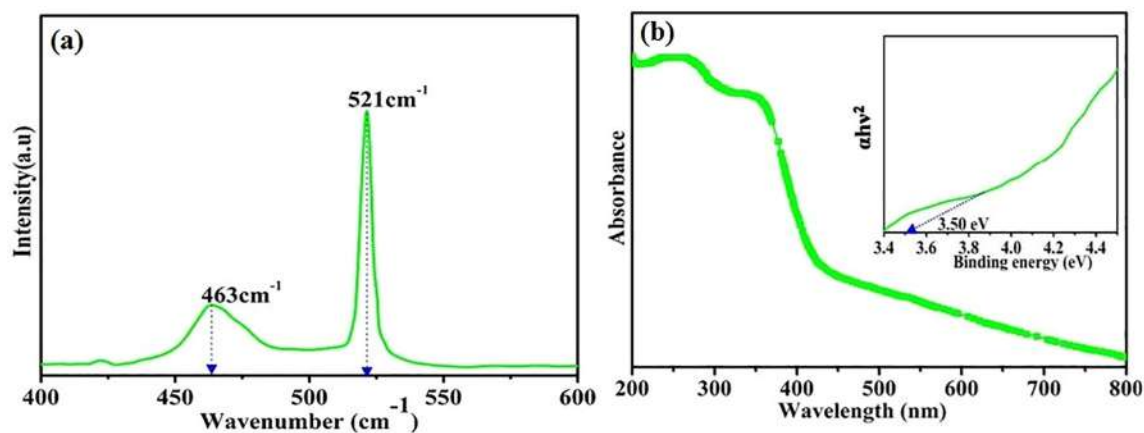
3.1. X-ray diffraction and infrared spectroscopy of CeO₂ NPs

A Fig. 1a shows the crystalline structure of fabricated CeO₂ NPs. The 2θ values of diffraction peaks were observed at 47.42, 28.51, and 33.06 matched with (2 2 0), (1 1 1), and (2 0 0) planes of the material. Correspondingly, erstwhile peaks were obtained at 2θ values of 78.99, 76.57, 69.00, 59.09, and 56.30 are analogous to (4 2 0), (3 3 1), (4 0 0), (2 2 2), and (3 1 1) planes of CeO₂ material. Off course, CeO₂ materials perfectly matched with JCPDS card no. 34-0394 and revealed a face centre cubic structure [27]. The recorded full width at half maxima of these peaks which are interpreted to determine the average crystalline size of synthesised NPs by using standard equation. An average crystalline size of CeO₂ NPs was found as 33.31 nm.

Moreover, the material was recorded by FT-IR spectroscopy (Fig. 1b) to authenticate the chemical bonding. The strong band was obtained at 3425 and 1498 cm⁻¹ because of the O–H vibrational frequency of hydration molecules contaminated during analysis [28–29]. A peak obtained at 1455 cm⁻¹ equivalent to the in-plane and out-of-plane bending of O–H bond exists in absorbed water molecule. The peak obtained at 1151 cm⁻¹ was responsible for the overtone bond for trace of the Ce-OH. The peaks were obtained at 862 and 957 cm⁻¹ were perfectly matched with bending vibrations of the Ce-O species. Finally, the peak achieved at below 862 cm⁻¹ indicated formation of the Ce-O bond [30].

3.2. Raman and UV-visible spectroscopy of CeO₂ NPs

Raman spectrum of material has been displayed in Fig. 2a. A cubic structure of cerium oxide nanoparticles was also confirmed by Raman spectroscopy. The stretching vibrational peak obtained at 463 cm⁻¹ due to the oxygen atoms. This renders the vibration very sensitive to micro-structural changes such as oxygen sub lattice disorder and non-stoichiometric [31]. A broaden and asymmetric peak obtained at 463 cm⁻¹ as the oxygen vacancy concentration increases, and the T_{2g} mode structure shifts to lower frequency. These changes may also be accompanied by the appear-

Scheme 1. Fabrication of CeO₂ NPs.Fig. 1. (a) XRD and (b) FT-IR patterns of synthesized CeO₂ NPs.Fig. 2. (a) Raman and (b) UV-visible spectrum of synthesized CeO₂ NPs.

ance of a strong longer peak at 521 cm⁻¹ which were attributed due to the O vacancies [31].

UV-visible spectroscopy was performed to understand the electronic structure and to estimate the optical band gap of material. The spectrum data of CeO₂ NPs have been shown in Fig. 2b. A

strong absorption band obtained at 370 nm was authenticated to the formation of desired material. Besides, in support of the present material a literature survey revealed that similar bands were observed in the earlier report [32]. A peak located at around 300–600 nm shifted towards shorter wave-length, which clearly

indicated that it might be due to the blue shift. Further, by using UV-visible data, band gap energy of material estimated around 3.50 eV. The band gap energy was estimated by plotting $(\alpha h\nu)^2$ of the micro-crystalline materials against the photon energy ($h\nu$). UV-absorption edge provided accountable guess of the band gap of any system.

3.3. Surface morphology of CeO₂ NPs

Morphological study of synthesized CeO₂ NPs was investigated by using SEM (Fig. 3). The study shows that high homogeneity emerged in the surface of the sample occur because of increasing the annealing temperature. The morphology of fabricated CeO₂ material shows spherical in shape at calcined 800 °C temperature. Also, data reveal nearly uniformity in spherical shapes with average diameter of each 60–85.1 nm (inset image in Fig. 3). Nearly uniform microspheres are shown in Fig. 3. In fact, these uniform microspheres emerged by aggregation of numerous nearly monodisperse nanospheres. Hence, the process of aggregation to spherical morphology caused by aging time, orientation, interaction, nucleation and extended heating at the higher temperature and fusion of nanoparticles, which lead to agglomeration that serves as crystal seed to grow the microspheres [33–35].

3.4. Antioxidant activity

In the past years, CeO₂ nanoparticles showed ROS scavenging capabilities that defence in gastrointestinal epithelium and human breast line models. A thorough study certainly shows that CeO₂ NPs with low Ce³⁺/Ce⁴⁺ surface ratios function as proficient antioxidant catalyse idiophone [36]. The DPPH scavenger radical method was broadly drawn to determine the proton donating capacity of synthesised CeO₂ NPs and to prevent the formation of free radicals. The DPPH scavenger radical method was utilized according to our previous work [37,38]. The scavenger free radical DPPH absorption plot was articulated to the green synthesized CeO₂ NPs from the extract contrasted with ascorbic acid as a positive control. We observed that CeO₂ NPs have the ability to remove DPPH free radicals as shown in Fig. 4. DPPH scavenger free radical activity was as concentration-dependent; as a result, the antioxidant property of synthesised NPs was increased when the concentration of NPs in a solution increased [39,40]. Also, the study showed CeO₂ NPs was more efficient than ascorbic acid.

3.5. Docking assay of CeO₂ NPs

3.5.1. Selection of inhibitor

Here our main aim is to develop an efficient inhibitor (material) against drug-resistant bacteria, therefore, we are working here to identify and develop inhibitors of essential biological pathways

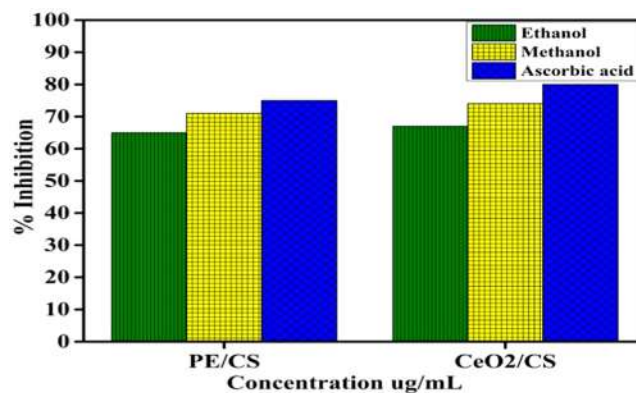


Fig. 4. Antioxidant property of plant extract (PE) and synthesized CeO₂ NPs.

that are not targeted by current therapies. A clinically pertinent antibacterial agent can be led by the fatty acid biosynthesis pathway [41,42]. Several small molecules were identified through a combination of high-throughput, besides, fragment screening was co-crystallized with β -ketoacyl-acyl carrier protein synthases III from *Escherichia coli* and *Streptococcus pneumoniae*. Structural-based drug design provided a new class of inhibitors. After optimization for gram-negative enzyme, inhibitory potency to study inhibition of an enzyme crystal structure of PDB ID 4Z8D which were targeted by inhibitor *trans*-4-[[[(2-chlorobenzyl) oxy] carbonyl] amino] methyl] cyclohexane carboxylic acid are listed in Fig. 5a [43]. The finalized 3D structures of the molecule were tested for global minima by ascertaining the minimum energy value of the molecule which was calculated as -9.65284 kcal/mole, and the same was replaced with the synthesized CeO₂ nanoparticles.

3.5.2. Molecular docking analysis

The interaction of nanoparticles with cells, DNA and protein has extensively acquired an immense interest in the field of bio-nanosciences. Fig. 6a shows the molecular docking of material. Fig. 6b-c exhibits the docking results of CeO₂ NPs with a size of 1.5 and 1 nm (PDB ID 4Z8D) correspondingly. An energy values for larger and smaller CeO₂ NPs clusters was calculated in the form of binding energies which were found as -651.85 and -540.90 kcal/mol respectively. The molecular docking study demonstrated the superior binding affinity for bigger clusters. The docked images of CeO₂ NPs are displayed in Fig. 6 (a-f) respectively and CeO₂ NPs of 1.5 nm with interacting close amino acid residues 247 ASN, with close distances of 1.201482, 1.449510, 2.118387, 1.984162, and 1.20254 in Å (Armstrong) are shown in Fig. 6c. The molecular docking study of synthesized CeO₂ NPs was explored with a fine harmony and the plot of accessible surface area and experimental data.

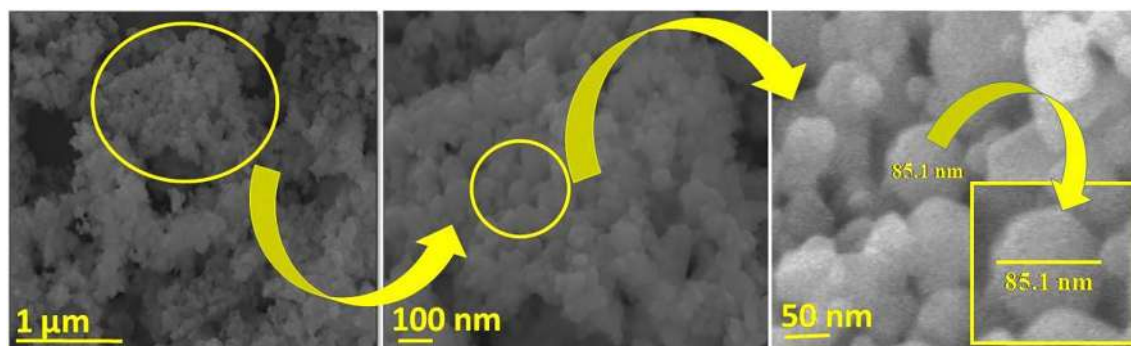


Fig. 3. SEM image of synthesized CeO₂ NPs.

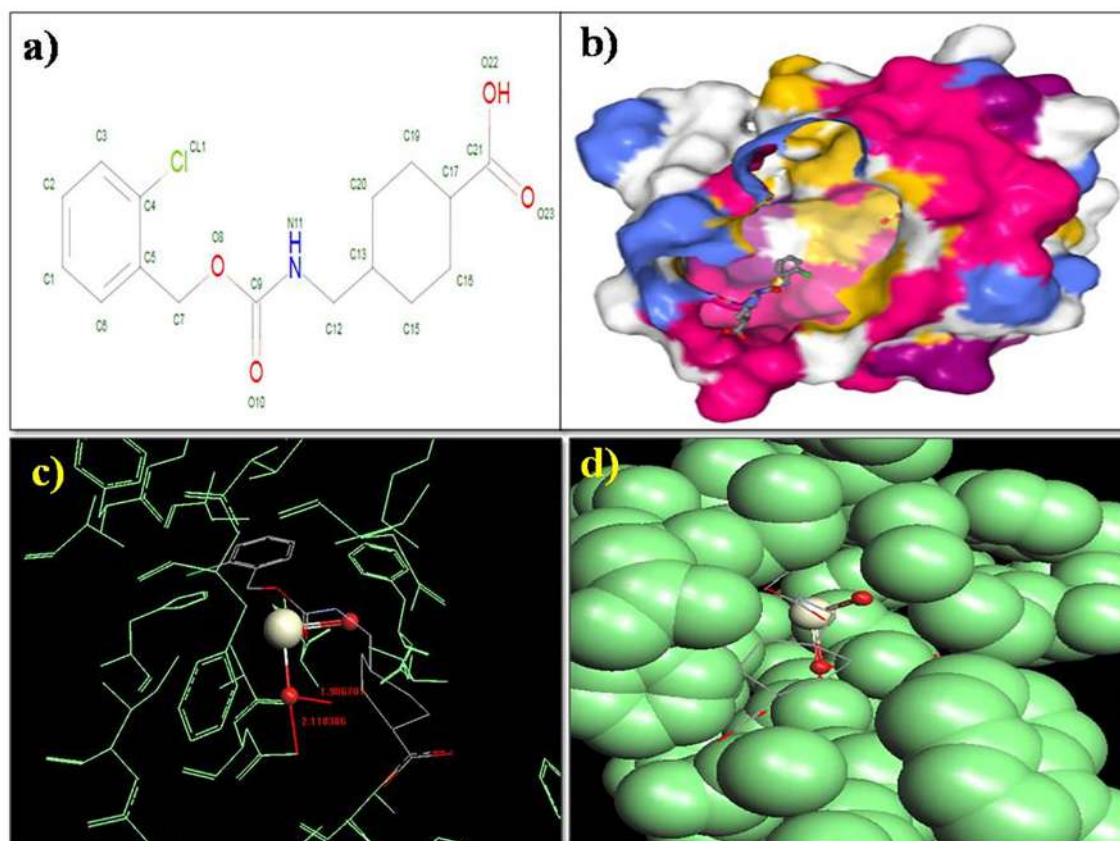


Fig. 5. (a) *trans*-4-(((2-chlorobenzyl)oxy)carbonyl)amino)methyl)cyclohexanecarboxylic acid; (b) 3-D Interaction of protein crystal structure PDB ID 4Z8D Natural inhibitor ligand code 4LBin center ball and stick surface mode; (c) 3-D ball and stick model of CeO₂ Nanoparticle fit in wireframe binding site, and (d) 3-D CeO₂ ball and stick mode fit in center CPK bonding site [43].

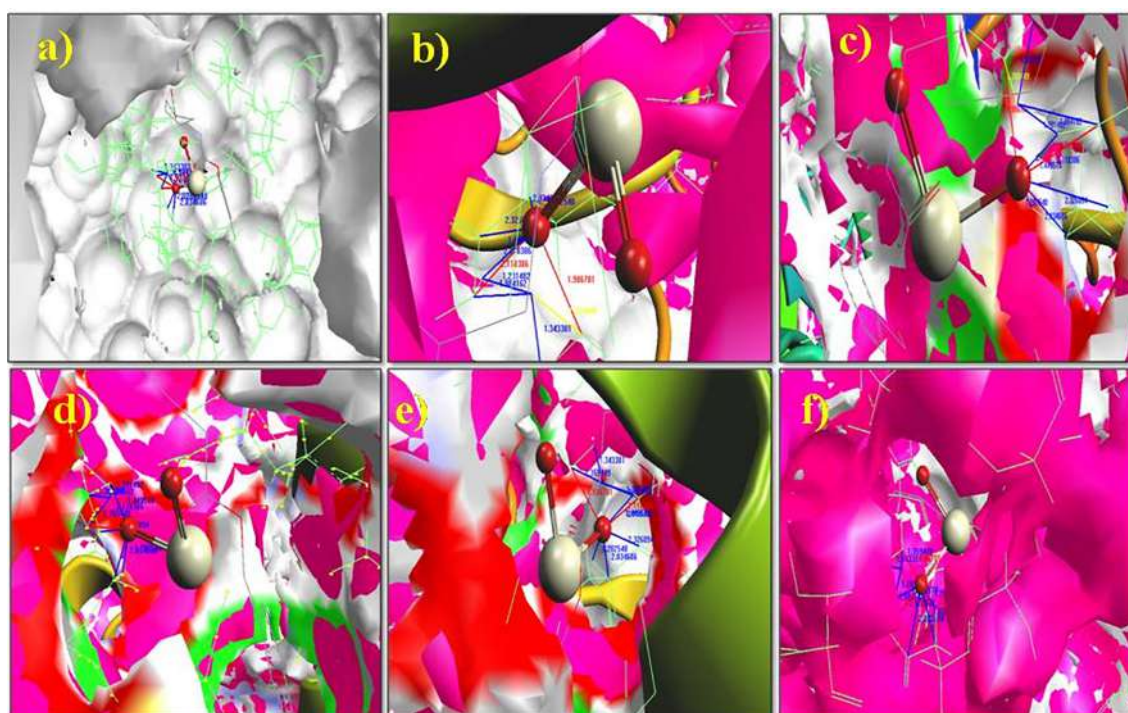


Fig. 6. (a-f) Protein crystal structures of PDB ID 4Z8D complex with CeO₂ as inhibitor red in centre ball and stick mode. Hydrogen bonds (2.5–3.5 Å) are depicted as blue, red lines in translucent surface cartan mode binding site show specific mode of interaction with selected amino acids residues. (For interpretation of the references to colour in this figure legend, the reader is referred to the web version of this article.)

4. Conclusion

In short, the *Cleome simplicifolia* assisted CeO₂ NPs which is authenticated by the XRD technique and resembles to a cubic structure. The crystallite size of CeO₂ NPs is estimated around 33.31 nm by Scherer equation. The morphology investigation of material has revealed spherical shapes with nearly monodisperse having average diameter of each 60–85.1 nm. Antioxidant activity of CeO₂ nonmaterial has demonstrated a more effective and an excellent activity against ascorbic acid. Moreover, the molecular docking study of material has shown an outstanding result with high binding energies –651.85 and –540.90 kcal/mol, and has revealed a greater binding affinity towards big clusters.

CRedit authorship contribution statement

Prashant B. Chouke: Investigation, Writing. **Rina D. Bagade:** Investigation, Writing. **Ajay K. Potbhare:** Methodology, Data Analysis. **Kanhaiya K. Dadurre:** Methodology, Data Analysis. **Ratiram Gomaji Chaudhary:** Conceptualization.

Declaration of Competing Interest

The authors declare that they have no known competing financial interests or personal relationships that could have appeared to influence the work reported in this paper.

Acknowledgements

The authors are thankful to the host institute for providing them research facilities. The authors would also like to thank Dr. Subhash Somkuvar for taking efforts in identification of the plant and its taxonomical investigation.

References

- [1] J.A. Vassie, J.M. Whitelock, M.S. Lord, Mol. Pharm. 15 (2018) 994–1004.
- [2] Z. Cao, C. Stowers, L. Rossi, W. Zhang, L. Lombardini, X. Ma, Environ. Sci. Nano. 4 (2017) 1086–1094.
- [3] S. Das, J.M. Dowding, K.E. Klump, J.F. McGinnis, W. Self, S. Seal, Nanomed. 8 (2013) 1483–1508.
- [4] K.M. Poole, C.E. Nelson, R.V. Joshi, J.R. Martin, M.K. Gupta, S.C. Haws, T.E. Kavanaugh, M.C. Skala, C.L. Duval, Biomaterial. 41 (2015) 166–175.
- [5] M.S. Gul, S. Ahmad, A. Naqvi, R. Hussain, A.A. Wali, I.A. Farooqi, J. Appl. Biol. Biotechnol. 5 (2017) 072–085.
- [6] H. Li, G. Lu, D. Qiao, Y. Wang, Y. Guo, Y. Guo, Catal. Lett. 141 (2011) 452–458.
- [7] M. Farahmandjou, M. Zarinkamar, T.P. Firoozabadi, Rev. Mex. Fis. 62 (2016) 496–499.
- [8] V.D. Araujo, W. Avansi, H.B. deCarvalho, M.L. Moreira, E. Longo, C. Ribeiro, M.I. B. Bernardi, Cryst. Eng. Comm. 14 (2012) 1150–1154.
- [9] T. Masui, H. Hirai, N. Imanaka, G. Adachi, T. Sakata, H. Mori, J. Mater. Sci. Lett. 21 (2002) 489–491.
- [10] S. Shao-Ju, B. Konstantin, Li-Jr. Borisenko, Yi-C. Chin, J. Nano. Res. 12 (2010) 1553–1559.
- [11] D.V. Pinjari, A.B. Pandit, Ultrason. Sonochem. 18 (2011) 1118–1123.
- [12] M. Darroudi, M.B. Ahmad, A.H. Abdullah, N.A. Ibrahim, Int. J. Nanomed. 6 (2011) 569–574.
- [13] P. Raveendran, J. Fu, S.L. Wallen, Am. Chem. Soc. 125 (2003) 13940–13941.
- [14] A.K. Potbhare, R.G. Chaudhary, P.B. Chouke, S. Yerpude, A. Mondal, V.N. Sonkusare, A.R. Rai, H.D. Juneja, Mater. Sci. Eng. C. 99 (2019) 783–793.
- [15] S. Narayanan, B.N. Sathy, U. Mony, M. Koyakutty, S.V. Nair, D. Menon, ACS Appl. Mater. Interface. 4 (2012) 251–260.
- [16] A.S. Karakoti, S.V. Kuchibhatla, K.S. Babu, J. Phys. Chem. C. 111 (2007) 17232–17240.
- [17] J. Gagnon, K.M. Fromm, Eur. J. Inorg. Chem. 27 (2015) 4510–4517.
- [18] Z. Tian, J. Li, Z. Zhang, W. Gao, X. Zhou, Y. Qu, Biomaterials. 59 (2015) 116–124.
- [19] A. Arya, A. Gangwar, S.K. Singh, Int. J. Nanomed. 11 (2016) 1159–1173.
- [20] X. Beaudoux, M. Virot, T. Chave, G. Durand, G. Leturcq, S.I. Nikitenko, Green Chem. 18 (2016) 3656–3668.
- [21] M.B. Gawande, V.B. Bonifacio, R.S. Varma, Green Chem. 15 (2013) 1226–1231.
- [22] S. Munusamy, K. Bhagyaraj, L. Vijayalakshmi, A. Stephen, V. Narayanan, Int. J. Innov. Res. Sci. Eng. 2 (2014) 318–323.
- [23] Q. Maqbool, M. Nazar, S. Naz, et al., Int. J. Nanomed. 11 (2016) 5015–5025.
- [24] G.S. Priya, A. Kanneganti, K.A. Kumar, K.V. Rao, S. Bykkam, Int. J. Sci. Res. Publ. 4 (6) (2014) 1–4.
- [25] N. Thovhogi, A. Diallo, A. Gurib-Fakim, M. Maaza, J. Alloys Compd. 647 (2015) 392–396.
- [26] A.R. Bagade, R.G. Chaudhary, A. Potbhare, A. Mondal, M. Desimone, K. Dadure, R. Mishra, H. Juneja, Chem. Select. 4 (2019) 6233–6244.
- [27] T.K. Mishra, A. Kumar, S.K. Sinha, B. Gupta, Mater. Today: Proc. 5 (2018) 27786–27794.
- [28] J. Tanna, R.G. Chaudhary, N. Gandhare, A. Mondal, H. Juneja, J. Chin. Adv. Mater. Soc. 5 (2017) 103–117.
- [29] V.N. Sonkusare, R.G. Chaudhary, G.S. Bhusari, A. Mondal, A.K. Potbhare, R.K. Mishra, H.D. Juneja, A.A. Abdala, ACS Omega. 5 (2020) 7823–7835.
- [30] S. Sebastiammal, A. Mariappan, K. Neyvasagam, A. Lesly Fathima, Mater. Today: Proc. 9 (2019) 627–632.
- [31] D.W. Wheeler, I. Khan, Vib. Spectrosc. 70 (2014) 200–206.
- [32] M.M. Ali, H.S. Mahdi, A. Parveen, A. Azam, AIP Conf. Proc. 1953 (2018) 030044–1–030044-4.
- [33] R.G. Chaudhary, V. Sonkusare, G. Bhusari, A. Mondal, D. Shaik, H. Juneja, Res. Chem. Intermed. 44 (2017) 2039–2060.
- [34] J. Tanna, R.G. Chaudhary, N. Gandhare, A. Rai, S. Yerpude, H. Juneja, J. Expt. Nanosci. 11 (2016) 884–900.
- [35] V. Sonkusare, R.G. Chaudhary, G. Bhusari, A. Rai, H. Juneja, Nano-Struct. Nano-Obj. 13 (2018) 121–131.
- [36] T. Pirmohamed, J.M. Dowding, S. Singh, B. Wasserman, E. Heckert, A.S. Karakoti, J.E. King, S. Seal, W.T. Self, Chem. Comm. 46 (2010) 2736–2738.
- [37] P.B. Chouke, A.K. Potbhare, G.S. Bhusari, S. Somkuvar, D.P.M.D. Shaik, R.K. Mishra, R.G. Chaudhary, Adv. Mater. Lett. 10 (2019) 355–360.
- [38] A.K. Potbhare, P.B. Chauke, S. Zahra, V. Sonkusare, R. Bagade, M. Ummekar, R.G. Chaudhary, Mater. Today: Process. 15 (2019) 454–463.
- [39] F. Pagliari, C. Mandoli, G. Forte, ACS Nano. 6 (2012) 3767–3775.
- [40] S.S. Lee, W. Song, M. Cho, ACS Nano. 26 (2013) 9693–9703.
- [41] X.Y. Lu, J. Tang, Z. Zhang, K. Ding, Curr. Med. Chem. 22 (2015) 651–667.
- [42] V. Gerasz, Annu. Rep. Med. Chem. 45 (2010) 295–311.
- [43] D.C. McKinney et al., ACS Infect. 2 (7) (2016) 456–464.